Research Article

Cancer Immunology Research

Anti–CTLA-4 Activates Intratumoral NK Cells and Combined with IL15/IL15Rα Complexes Enhances Tumor Control

Emilio Sanseviero[1], Erin M. O'Brien[1], Jenna R. Karras[1], Tamer B. Shabaneh[2,3], Bulent Arman Aksoy[4], Wei Xu[5], Cathy Zheng[5], Xiangfan Yin[6], Xiaowei Xu[5], Giorgos C. Karakousis[5], Ravi K. Amaravadi[5], Brian Nam[7], Mary Jo Turk[2,3], Jeff Hammerbacher[4], Mark P. Rubinstein[4,8], Lynn M. Schuchter[5], Tara C. Mitchell[5], Qin Liu[6], and Erica L. Stone[1]

Abstract

Antibodies targeting CTLA-4 induce durable responses in some patients with melanoma and are being tested in a variety of human cancers. However, these therapies are ineffective for a majority of patients across tumor types. Further understanding the immune alterations induced by these therapies may enable the development of novel strategies to enhance tumor control and biomarkers to identify patients most likely to respond. In several murine models, including colon26, MC38, CT26, and B16 tumors cotreated with GVAX, anti–CTLA-4 efficacy depends on interactions between the Fc region of CTLA-4 antibodies and Fc receptors (FcR). Anti–CTLA-4 binding to FcRs has been linked to depletion of intratumoral T regulatory cells (Treg). In agreement with previous studies, we found that Tregs infiltrating CT26, B16-F1, and autochthonous $Braf^{V600E}Pten^{-/-}$ melanoma tumors had higher expression of surface CTLA-4 (sCTLA-4) than other T-cell subsets, and anti–CTLA-4 treatment led to FcR-dependent depletion of Tregs infiltrating CT26 tumors. This Treg depletion coincided with activation and degranulation of intratumoral natural killer cells. Similarly, in non–small cell lung cancer (NSCLC) and melanoma patient-derived tumor tissue, Tregs had higher sCTLA-4 expression than other intratumoral T-cell subsets, and Tregs infiltrating NSCLC expressed more sCTLA-4 than circulating Tregs. Patients with cutaneous melanoma who benefited from ipilimumab, a mAb targeting CTLA-4, had higher intratumoral CD56 expression, compared with patients who received little to no benefit from this therapy. Furthermore, using the murine CT26 model we found that combination therapy with anti–CTLA-4 plus IL15/IL15Rα complexes enhanced tumor control compared with either monotherapy.

Introduction

Combination therapy with immune checkpoint inhibitors targeting PD-1 (i.e., nivolumab) and CTLA-4 (i.e., ipilimumab) for advanced melanoma is dramatically successful with up to a 60% response rate (1), and combination therapy with nivolumab and ipilimumab leads to higher response rates than nivolumab alone in patients with brain metastases (2). Likewise, clinical trials have shown efficacy of combination therapy with nivolumab and ipilimumab in a subset of patients with renal cell carcinoma and non–small cell lung cancer (NSCLC; refs. 3, 4). However, for a majority of patients across tumor types, immunotherapies are ineffective. Thus, a major goal in tumor immunology is to further understand the immunomodulation induced by these therapies. This will enable the development of novel therapeutic strategies to enhance responses and foster development of biomarkers to identify patients most likely to respond to specific therapies.

Immune checkpoint inhibitors are designed to prevent the interaction of checkpoint molecules with their ligands, and thus prevent immune inhibition. However, in addition to blocking activity, some antibodies can mediate effector functions when their Fc domain interacts with Fc receptors (FcR). In murine models, anti–CTLA-4 can lead to the death of cells expressing CTLA-4 on their cell surface in an Fc/FcR-dependent manner (5–10). Although

[1]Immunology, Microenvironment and Metastasis Program, Wistar Cancer Center, The Wistar Institute, Philadelphia, Pennsylvania. [2]Norris Cotton Cancer Center, Dartmouth-Hitchcock Medical Center, Lebanon, New Hampshire. [3]Department of Microbiology and Immunology, Geisel School of Medicine at Dartmouth, Hanover, New Hampshire. [4]Department of Microbiology and Immunology, Medical University of South Carolina, Charleston, South Carolina. [5]Melanoma Program, Abramson Cancer Center, University of Pennsylvania, Philadelphia, Pennsylvania. [6]Molecular and Cellular Oncogenesis Program, Wistar Cancer Center, The Wistar Institute, Philadelphia, Pennsylvania. [7]The Helen F. Graham Cancer Center & Research Institute, Christiana Care Health System, Newark, Delaware. [8]Department of Surgery, Medical University of South Carolina, Charleston, South Carolina.

Note: Supplementary data for this article are available at Cancer Immunology Research Online (http://cancerimmunolres.aacrjournals.org/).

E. Sanseviero and E.M. O'Brien contributed equally to this article.

Current address for E.M. O'Brien: Drexel University, School of Biomedical Engineering, Philadelphia, Pennsylvania; and current address for E.L. Stone: GigaGen, Inc., South San Francisco, California.

Corresponding Author: Erica L. Stone, GigaGen, 1 Tower Place, Suite 750, South San Francisco, CA 94080. Phone: 978-853-3529; Fax: 650-332-1105; E-mail: estone@gigagen.com

Cancer Immunol Res 2019;7:1371–80

doi: 10.1158/2326-6066.CIR-18-0386

CTLA-4 is largely intracellular, it is expressed on the surface of regulatory T cells (Treg) infiltrating murine tumor models (5–7), and anti–CTLA-4 has been shown to be able to mediate depletion of these intratumoral Tregs. In these models anti–CTLA-4–mediated depletion of intratumoral Tregs correlates with antitumor activity of anti–CTLA-4 (5–7). In B16 tumor–bearing mice treated with a GM-CSF–secreting vaccine, Treg depletion has been linked to FcRs on macrophages and nonclassical monocytes (5). However, GM-CSF may induce intratumoral accumulation and activation of myeloid-derived suppressor cells in addition to macrophages and nonclassical monocytes. Natural killer (NK) cells are also able to mediate the depletion of antibody opsonized cells in an FcR-dependent manner. Thus, additional studies are necessary to determine the effect of anti–CTLA-4 on intratumoral NK cells. Such studies may suggest combination strategies likely to enhance the efficacy of anti–CTLA-4 therapies.

In part, because Tregs are not reduced in the blood of patients receiving anti–CTLA-4 antibodies (11–13), it has been thought that antibody-dependent cell-mediated cytotoxicity (ADCC)-mediated depletion of Tregs is not a mechanism of action of anti–CTLA-4 in patients. However, in murine models, intratumoral Tregs have higher surface CTLA-4 (sCTLA-4) expression compared with peripheral Tregs, and anti–CTLA-4 specifically depletes intratumoral Tregs but not peripheral Tregs (5, 7, 13). It has been found that ipilimumab, a human IgG1 antibody, can induce ADCC of Tregs, and reduced intratumoral Tregs following ipilimumab treatment may correlate with efficacy in patients (12, 14). In addition, in patients with tumors with a high mutation burden, the response to ipilimumab is associated with the presence of the high-affinity CD16-V158F germline SNP (8). Despite these data the ability of ipilimumab to deplete intratumoral Tregs in patients remains controversial. Therefore, further investigations are required to determine whether Tregs infiltrating tumors in patients also express higher amounts of sCTLA-4, which would provide a rationale for how anti–CTLA-4 therapies specifically deplete intratumoral Tregs in patients.

Here we show that Tregs infiltrating patient-derived NSCLC tissue expressed more sCTLA-4 than Tregs from matched patient blood or intratumoral effector T cells. Similarly, in a majority of patient-derived melanoma tissue, intratumoral Tregs express more sCTLA-4 than effector T cells. Using the CT26 murine tumor model we found that anti–CTLA-4 therapies induced NK-cell activation and degranulation specifically within the tumor microenvironment. This NK-cell activation coincided with depletion of intratumoral Tregs. Furthermore, combination of anti–CTLA-4 plus IL15/IL15Rα complexes enhanced tumor control in comparison with either monotherapy. Consistently, patients who benefited from ipilimumab had higher intratumoral expression of the NK-cell marker, CD56.

Materials and Methods

Study approval

Patient studies were conducted in accordance with ethical guidelines including the Declaration of Helsinki, The Belmont Report, and the U.S. Common Rule. Patient-derived tumor tissue specimens were collected in accordance to the Institutional Review Boards at HFGCC of Christiana Health Care System (NSCLC, Newark, DE) or The University of Pennsylvania (melanoma, Philadelphia, PA). Informed consent was received from participants prior to inclusion in the study.

Mice

Murine experiments were approved by the Institutional Animal Care and Use Committees of The Wistar Institute (Philadelphia, PA) or Dartmouth University (Hanover, NH). C57BL/6J mice were obtained from The Jackson Laboratories and BALB/C mice were obtained from Taconic, and kept under specific pathogen-free condition in The Wistar Institute's Animal Facility (Philadelphia, PA).

Unless otherwise indicated, 5×10^5 CT26 tumor cells in 200 μL of PBS were subcutaneously transplanted into the right flank of mice using 27g needles. A total of 2.5×10^5–5×10^5 YUMM1.7 cells or 1×10^6 B16-F1 cells were transplanted subcutaneously on day 0 where indicated. In experiments in which mice were treated with anti–CTLA-4, unless otherwise noted, mice were treated with 300 μg of the indicated anti–CTLA-4 clone or appropriate isotype (both from BioXCell) diluted in PBS, and mice were euthanized 5 days post-anti–CTLA-4 administration for analysis of intratumoral T cells. Where indicated, mice were injected intravenously with 200 μg of anti-FcγRIV (clone 9E9) 1 hour prior to injection of anti–CTLA-4. Where indicated, mice were treated intraperitoneally on days 6 and 8 with 200 μL IL15/IL15Rα complexes, containing 0.5 μg human IL15 (NCI biorepository) and 2.33 μg of soluble murine IL15Rα-Fc (R&D Systems/Thermo Fisher Scientific) per dose, and on days 9, 12, 15, and 17 with 200 μg anti–CTLA-4 (clone 9D9). After treatment initiation, tumor size was measured every 2 to 4 days and mice were euthanized when tumors reached 12×12 mm^2. In experiments in which tumor-bearing mice were euthanized at a set timepoint, tumors were weighed upon euthanasia.

Induction of autochthonous tumors

Tyr::*CreER*$^+$*Braf*$^{CA/+}$*Pten*$^{fl/fl}$ [*Braf*^{tm1Mmcm} *Pten*^{tm1Hwu} Tg(Tyr-cre/ERT2)13Bos/BosJ] mice were kindly provided by Marcus Bosenberg (Yale University, New Haven, CT), and bred at Dartmouth University onto a C57BL/6 background, with >98% purity confirmed by congenic testing (DartMouse). For induction of autochthonous tumors, 80 μg of 4-hydroxy-tamoxifen (Sigma) in DMSO was intradermally injected in the right flanks of 4-week-old mice. Tumors and skin samples from age-matched mice were harvested 5 weeks later.

Flow cytometry

Tumors were extracted, minced, and digested in 5 mL HBSS with 0.5% FBS and 1% HEPES containing 1 mg/mL collagenase type-I from *Clostridium histolyticum* (Sigma-Aldrich) for 30 minutes at 37°C. Cells were then washed and filtered through 70-μm cell strainers.

Autochthonous tumors and murine skin samples were harvested, minced, and digested for 45 minutes at 37°C in 2 mL HBSS containing 7 mg/mL collagenase D (Roche) and 200 μg/mL DNase I (Roche), using magnetic bar stirring at 300 RPM. Tissue fragments were mechanically dissociated through a 40-μm nylon mesh filter. Samples were washed in RPMI1640 media containing 10% FBS and 2 mmol/L EDTA.

For sCTLA-4 staining, cells were processed as before, stained with antibodies to surface antigens, including CTLA-4 or isotype control, and then two rounds of FASER-PE (Miltenyi Biotec) staining were performed according to the manufacturer's instructions. For mouse FcR staining, cell suspensions were incubated with anti-mouse FcγRIV (CD16.2, clone 9E9, BioLegend) for 20 minutes at 4°C, washed twice, incubated with anti-mouse

CD16/32 (clone 2.4G2, BD Bioscience) for 10 minutes at 4°C, then stained with all the other surface antibodies. Fixation and intracellular staining was accomplished with eBioscience FOXP3 Transcription Factor Staining Buffer Set.

Patient-derived tumor tissues were minced into pieces approximately 2 × 2 mm and processed with human Tumor Dissociation Kit (Miltenyi Biotec) according to the manufacturer's instructions. Red blood cell lysis buffer (eBioscience) was used to remove red blood cells from blood specimens. FcRs were blocked with FcR Blocking Reagent (Miltenyi Biotec), and then cells were stained similarly to murine cells. Patient-derived tissues were processed for flow cytometry the day of excision.

Samples were analyzed using LSR IIs (BD Bioscience) equipped with four lasers, a CELESTA (BD Bioscience) flow cytometer equipped with three lasers, or a Gallios Flow Cytometer (Beckman Coulter). Mean fluorescence intensity (MFI) indicates geometric mean of the indicated fluorescence. Data were analyzed using FlowJo versions 9 or 10 (TreeStar).

Generation and testing of IL15/IL15Rα complexes

IL15/IL15Rα complexes were generated by combining 0.5 μg human IL15 (NCI biorepository) with 2.33 μg of soluble murine IL15Rα-Fc (R&D Systems/Thermo Fisher Scientific) per dose for 30 minutes at 37°C. PBS was used to quantum satis (q.s.) IL15 complexes to 200 μL per dose; doses were aliquoted and stored at −80°C. Batches of IL15 complexes were validated once by intraperitoneally injecting a mouse with IL15 complexes containing 0.5 μg human IL15 (NCI biorepository) and 2.33 μg of soluble murine IL15Rα-Fc (R&D Systems/Thermo Fisher Scientific) per dose on days 1, 3, and 5. On day 7, spleens from mice treated with IL15 complexes were then analyzed for size, NK-cell frequency, and frequency of activated $CD8^+$ T cells compared with control spleen.

Analysis of RNA-seq data

Relative expression of the NK-cell genes *NCAM1* (CD56), *FCGR3A*, *NCR1*, *NCR2*, and *KLRK1*, and the T cell and myeloid genes *CD3D*, *CD8A*, *CD4*, *CD14*, *CD74*, *CD163*, and *CX3CR1* in melanoma tissue from patients who received benefit or little to no benefit from anti–CTLA-4 published by Snyder and colleagues (2014) or Van Allen and colleagues (2015) were compared. *NCAM1* expression in melanoma tissue from patients who received benefit or little to no benefit from anti–CTLA-4 as published by Snyder and colleagues (2014) was chosen for further analysis. Statistical difference in expression of *NCAM1* was only found when analysis was restricted to samples from cutaneous melanoma.

Statistical analysis

Prism 7 (GraphPad) was used for statistical data analysis. To determine statistical significance, paired or two-group Student *t* test was used as indicated. For multiple groups of data analysis, ANOVA with Tukey *post-hoc* multiple comparison was used to determine statistical significance between two groups. For comparisons of multiple groups to a single group, Dunnett *post-hoc* multiple comparisons test was used to determine statistical significance. For data that did not follow normal distribution, Wilcoxon rank-sum test was used to determine statistical significance. To determine if indicated treatments induced significant difference in tumor progression, the velocities of tumor growth were compared between groups using a linear mixed effects model with the random effect at mouse level. A likelihood ratio testing nested models (with versus without the interaction term of treatment with follow-up days) was used to examine if tumor growth slopes are significantly different between treatments in overall. $P < 0.05$ was considered statistically significant.

Results

Anti–CTLA-4 induces NK-cell activation in the tumor microenvironment

As expected, administration of anti–CTLA-4 clone 9H10, a Syrian hamster IgG, to mice bearing CT26 tumors, an anti–CTLA4–responsive murine colorectal tumor model, led to depletion of Tregs specifically within the tumor microenvironment (Fig. 1A). Anti–CTLA-4 clone 9H10 has been shown to bind to FcγRIV, and mediate depletion of Tregs infiltrating B16 tumors in an FcγRIV-dependent manner (5). This and other data suggest that anti–CTLA-4–induced depletion of intratumoral Tregs may be mediated by nonclassical monocytes (5, 14). Furthermore, we found that pretreatment with an antibody to FcγRIV (clone 9E9), which has been reported to be a blocking antibody, prevented anti–CTLA-4–mediated depletion of Tregs infiltrating CT26 tumors (Fig. 1B). We note, however, that to our knowledge, the ability of anti-FcγRIV clone 9E9 to deplete FcγRIV-expressing cells has not been investigated, and thus a possibility is that administration of FcγRIV depleted $Fc\gamma RIV^+$ cells, which may also express other FcRs. Nonetheless, our data further support the now prevailing evidence that anti–CTLA-4 clone 9H10 depletes intratumoral Tregs in an FcR-dependent manner.

NK cells also express FcRs and are able to mediate FcR-dependent functions of antibodies. Thus, we investigated the effect of anti–CTLA-4 treatment on NK cells. We found that, 5 days postadministration of a single dose of anti–CTLA-4 clone 9H10, an increased frequency of intratumoral NK cells were activated, as measured by NK-cell expression of CD69 and SCA1 (Fig. 1C and D). However, NK-cell activation appeared to be limited to the tumor microenvironment, as the frequency of activated NK cells was not increased outside of the tumor microenvironment (Fig. 1C). Thus, anti–CTLA-4 led to NK-cell activation specifically within the tumor microenvironment.

Anti–CTLA-4 induces NK-cell degranulation in the tumor microenvironment

As the binding of the Fc region of antibodies to activating FcRs on NK cells can lead to NK-cell activation, it is possible that anti–CTLA-4 bound to intratumoral Tregs activates NK cells to kill Tregs opsonized by anti–CTLA-4. In agreement with this we found that 3 days postadministration of a single dose of anti–CTLA-4 clone 9H10, a timepoint that correlates with Treg depletion (Fig. 1A; refs. 5, 6), an increased frequency of intratumoral NK cells displayed CD107a on their cell surface directly *ex vivo* (Fig. 1E; Supplementary Fig. S1A). Surface CD107a expression indicates that these NK cells have recently degranulated.

Although expression of FcγRIV on NK cells in the periphery is rare, a fraction of intratumoral NK cells in B6 mice do indeed express FcγRIV (5). Similarly, we found that although peripheral NK cells in BALB/c mice expressed little to no FcγRIV, approximately 20% of NK cells infiltrating CT26 tumors in BALB/c mice expressed FcγRIV (Fig. 1F and G). Furthermore, we found that $Fc\gamma RIV^+$ NK cells were present within tumors at a similar frequency to $Fc\gamma RIV^+$ neutrophils and monocytes (Fig. 1H). However, we note that the per cell expression of FcγRIV was

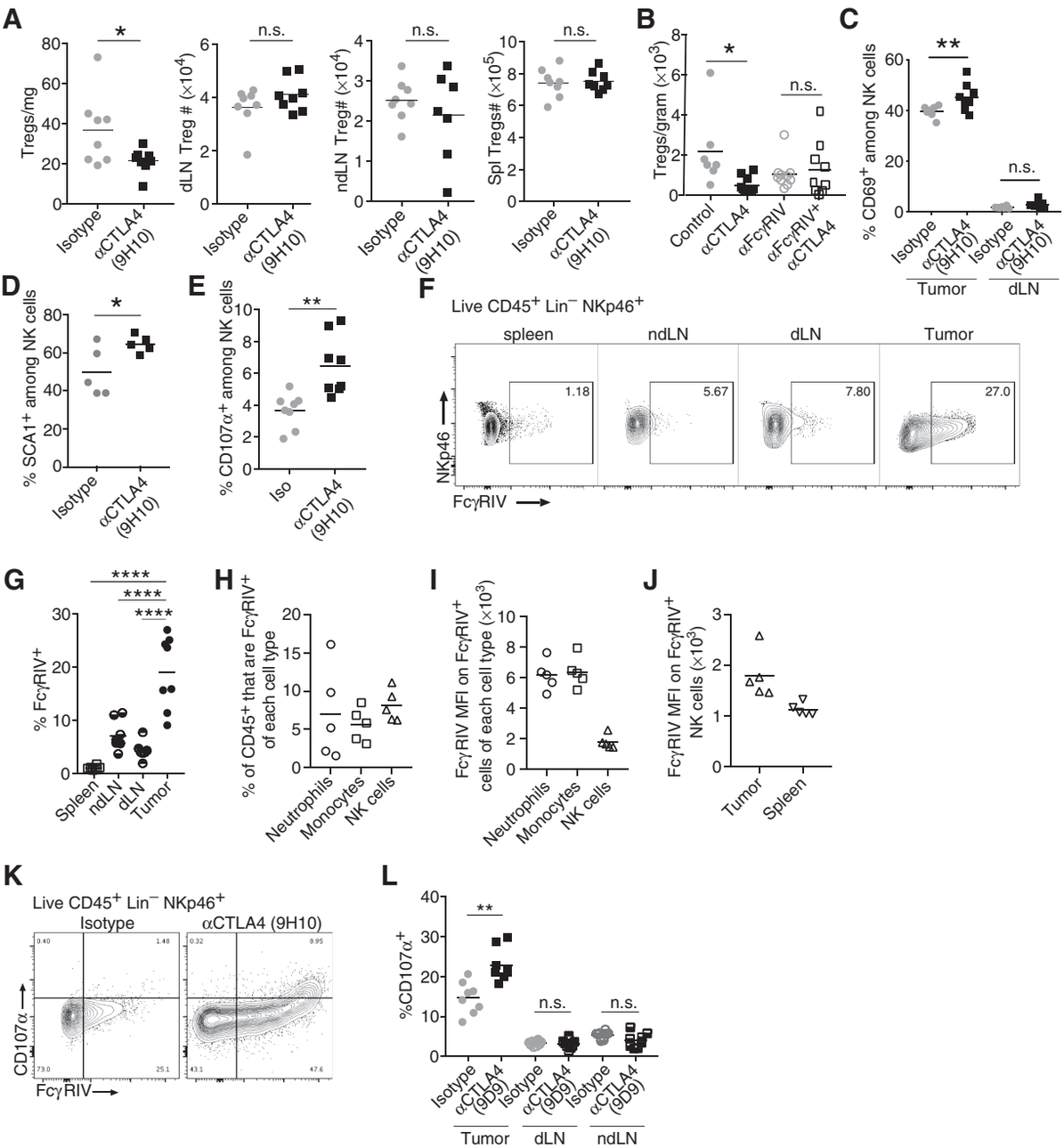

Figure 1.

Anti–CTLA-4 induces NK-cell activation and degranulation specifically in the tumor microenvironment. **A,** Twelve days posttransplantation of CT26 cells, mice were treated with anti–CTLA-4 (clone 9H10) or isotype (Isotype) control and 3 days later (day 15) the number of Tregs (live $CD45^+CD19^-CD11c^-Ly6G^-CD3^+CD4^+FOXP3^+$) per mg of tumor tissue or within the draining lymph node (dLN), a nondraining lymph node (ndLN), or the spleen (Spl) was determined by flow cytometry. Data are representative of three independent experiments. **B,** Seven days posttransplantation of CT26 tumors mice were intravenously injected with anti-FcγRIV (clone 9E9) or Armenian Hamster isotype control. One hour later anti–CTLA-4 clone 9H10 or Syrian Hamster isotype control was administered (intraperitoneally). On day 14, 5 days postadministration of antibodies, the number of Tregs (live $CD45^+$ $B220^-CD11b^-CD11c^-Ly6G^-CD3^+$) per gram of tumor tissue was determined by flow cytometry. Results are from one experiment. **C** and **D,** CT26 cells were transplanted subcutaneously and on the indicated day post tumor transplantation, mice were treated with anti–CTLA-4 (clone 9H10) or isotype (Isotype) control. **C,** Graphs show the frequency of NK cells (live $CD45^+NKp46^+$) within the tumor or dLN that expressed CD69 on day 15 when mice were treated with anti–CTLA-4 clone 9H10 on day 10. Data are representative of three independent experiments. **D,** Graphs show the frequency of NK cells (live $CD45^+CD19^-Ly6G^-CD3^-NKp46^+$) that expressed SCA1 on day 14 when mice were treated with anti–CTLA-4 clone 9H10 on day 9. Results are from one experiment with 5 mice per group. **E,** Graphs show the frequency of NK cells (live $CD45^+CD19^-CD11c^-Ly6G^-CD3^-NKp46^+$) that displayed CD107a on their surface when mice were treated with anti–CTLA-4 clone 9H10 on day 12. Data are representative of three independent experiments. Representative contour plots (**F**) and graph (**G**) showing expression of FcγRIV (CD16.2) on NK cells (live $CD45^+CD19^-CD11c^-Ly6G^-CD3^-NKp46^+$) from indicated organs 15 days after transplantation of CT26 tumors. Data are representative of three independent experiments. (*Continued on the following page.*)

significantly higher on intratumoral FcγRIV$^+$ neutrophils and monocytes than FcγRIV$^+$ NK cells (Fig. 1I). Nonetheless, the expression of FcγRIV$^+$ was increased on intratumoral FcγRIV$^+$ NK cells compared with splenic NK cells (Fig. 1J). Furthermore, consistent with the dependence of anti–CTLA-4 clone 9H10 on FcγRIV for intratumoral Treg depletion, surface CD107a$^+$ NK cells were largely FcγRIV$^+$ (Fig. 1K).

Anti–CTLA-4 clone 9H10 is a hamster anti-mouse IgG and thus may bind to FcRs differently than mouse anti-mouse IgG. Thus, to determine whether NK-cell activation following anti–CTLA-4 administration is specific to anti–CTLA-4 clone 9H10 or may be broadly applicable across anti–CTLA-4 therapies able to mediate ADCC, we investigated NK-cell phenotype following administration of anti–CTLA-4 clone 9D9, a murine IgG2b antibody. Murine antibodies of the IgG2b isotype are known to be able to induce NK-cell–mediated ADCC. As with anti–CTLA-4 clone 9H10, anti–CTLA-4 clone 9D9 led to NK-cell degranulation (Fig. 1L). Consistent with anti–CTLA-4–inducing Treg depletion specifically within the tumor microenvironment, the increase in NK-cell degranulation was specific to the tumor microenvironment (Fig. 1L).

NK cells infiltrating CT26 tumors express little to no CTLA-4

NK cells are able to express CTLA-4 when cultured in the presence of IL2 (15). Thus, a possibility was that anti–CTLA-4 activated NK cells by blocking CTLA-4 expressed by NK cells. To investigate this possibility, we used flow cytometry to assess surface and intracellular CTLA-4 expression by NK cells infiltrating CT26 tumors on day 18. As expected, we found that intratumoral Tregs expressed sCTLA-4; however, little to no CTLA-4 expression by NK cells was detected (Supplementary Fig. S1B). From these results we concluded it is unlikely that anti–CTLA-4 activated NK cells by relieving a "brake" imposed on NK cells by their own expression of CTLA-4.

In many murine tumor models Tregs express more sCTLA-4 than other T-cell subsets

The ability of anti–CTLA-4 to specifically mediate intratumoral Treg depletion (Fig. 1A) is consistent with intratumoral Tregs expressing more sCTLA-4 than peripheral Tregs (Supplementary Fig. S2A), and this has previously been shown of Tregs infiltrating B16-BL6 and CT26 tumor models (5, 6). In agreement with this, anti–CTLA-4 therapy leads to depletion of Tregs with the highest CTLA-4 expression (5, 6). However, activated effector T cells can also have CTLA-4 expression, and it has previously been found that CD4$^+$ effector T cells responding to chronic stimulation can further upregulate CTLA-4 (16). Furthermore, CTLA-4 surface retention can be enhanced by stimulation (17). In agreement with this, we found that sCTLA-4$^+$ Tregs and conventional CD4$^+$ T cells infiltrating well-established YUMM1.7 tumors, a transplanted *Braf*^{V600E}/*Pten*$^{-/-}$/*Cdkn2a*$^{-/-}$ melanoma model (18), expressed similar amounts of sCTLA-4 (Supplementary Fig. S2B). However, Tregs expressed significantly greater amounts of sCTLA-4 compared with other T-cell subsets infiltrating autochthonous melanomas in a conditionally induced *Braf*^{V600E}/*Pten*$^{-/-}$ melanoma mouse model (Supplementary Fig. S2C). Using this model we also found that melanoma infiltrating Tregs expressed more sCTLA-4 than peripheral or skin Tregs (Supplementary Fig. S2D). Nonetheless, these data demonstrate that in some tumor microenvironments, a portion of effector T cells may express sCTLA-4 at amounts similar to Tregs. Thus, as anti–CTLA-4 therapies that mediate ADCC-induced depletion of cells with the highest sCTLA-4 expression (5, 6), it was relevant to determine the relative sCTLA-4 expression by T-cell subsets infiltrating patient-derived tumor tissue.

Tregs express higher sCTLA-4 than effector T cells in patient-derived NSCLC tissue

Tregs infiltrating previously untreated patient–derived NSCLC tissue expressed higher amounts of intracellular CTLA-4 (IC CTLA-4) than other intratumoral T-cell subsets (Fig. 2A and B; ref. 8). The majority of CTLA-4 is intracellular (17, 19), and little is known about the expression of sCTLA-4 on T-cell subsets infiltrating patient-derived tumor tissue directly *ex vivo*. Using flow cytometry, we found that although nearly all Tregs infiltrating patient-derived NSCLC tissue expressed IC CTLA-4 (Fig. 2A), only a fraction (∼10%–65%) of intratumoral Tregs expressed sCTLA-4 (Fig. 2C). sCTLA-4$^+$ Tregs expressed more IC CTLA-4 and FOXP3 compared with sCTLA-4$^-$ Tregs (Fig. 2D and E). Nonetheless, a higher frequency of Tregs than CD8$^+$ or CD4$^+$ effector T cells infiltrating patient-derived NSCLC tissue expressed sCTLA-4 (Fig. 2C). In nearly all NSCLC tissues analyzed, sCTLA-4$^+$ Tregs expressed more sCTLA-4 on a per cell basis than the sCTLA-4$^+$ intratumoral CD8$^+$ or CD4$^+$ effector T cells from the same tumor tissue (Fig. 2F).

Tregs infiltrating NSCLC express higher sCTLA-4 compared with circulating Tregs

Tregs infiltrating patient-derived NSCLC tissue expressed more intracellular CTLA-4 than Tregs from matched patient blood (Fig. 3A and B; ref. 8). However, even in intratumoral Tregs the majority of CTLA-4 was intracellular. Thus, we compared sCTLA-4 expression on intratumoral and peripheral Tregs to better understand whether, similar to what has been found in murine models, Tregs infiltrating patient-derived tumor tissue express more sCTLA-4 than peripheral Tregs. These results could thus suggest, whether anti–CTLA-4 is likely to specifically target intratumoral Tregs in patients. Comparing the data from Fig. 2 to costained

(*Continued.*) **H,** Graph shows the frequency of live intratumoral CD45$^+$ cells that were FcγRIV$^+$ neutrophils (NKp46$^-$CD11B$^+$LY6G$^+$), monocytes (NKp46$^-$LY6G$^-$LY6C^{Hi}), and NK cells (CD3$^-$NKp46$^+$) 13 days posttransplantation of CT26 tumors. Data are representative of three independent experiments. FcγRIV MFI on FcγRIV$^+$ population of the indicated cell type within the tumor (**I**) or on intratumoral and splenic NK cells (**J**) 13 days posttransplantation of CT26 tumor cells. Data are representative of three independent experiments. **K,** Representative contour plots showing expression of FcγRIV versus CD107 on NK cells (live CD45$^+$CD19$^-$CD11c$^-$Ly6G$^-$NKp46$^+$) 3 days postadministration of anti–CTLA-4 clone 9H10. Data are representative of three independent experiments with at least 5 mice per group. **L,** Graphs show the frequency of NK cells (live CD45$^+$CD19$^-$CD11c$^-$Ly6G$^-$CD3$^-$NKp46$^+$) in indicated organs (ndLN, nontumor-draining lymph node) that expressed CD107a 5 days postadministration of anti–CTLA-4 clone 9D9. Data are representative of two independent experiments. To determine statistical significance, *t* test for two groups was used. For comparison between multiple groups in **C**, ANOVA with Tukey *post-hoc* for multiple comparisons, and for **G**, ANOVA with Dunnett *post-hoc* for multiple comparisons was used to determine statistical significance between two groups (n.s., nonsignificant; *, $P < 0.05$; **, $P < 0.01$; ****, $P < 0.0001$).

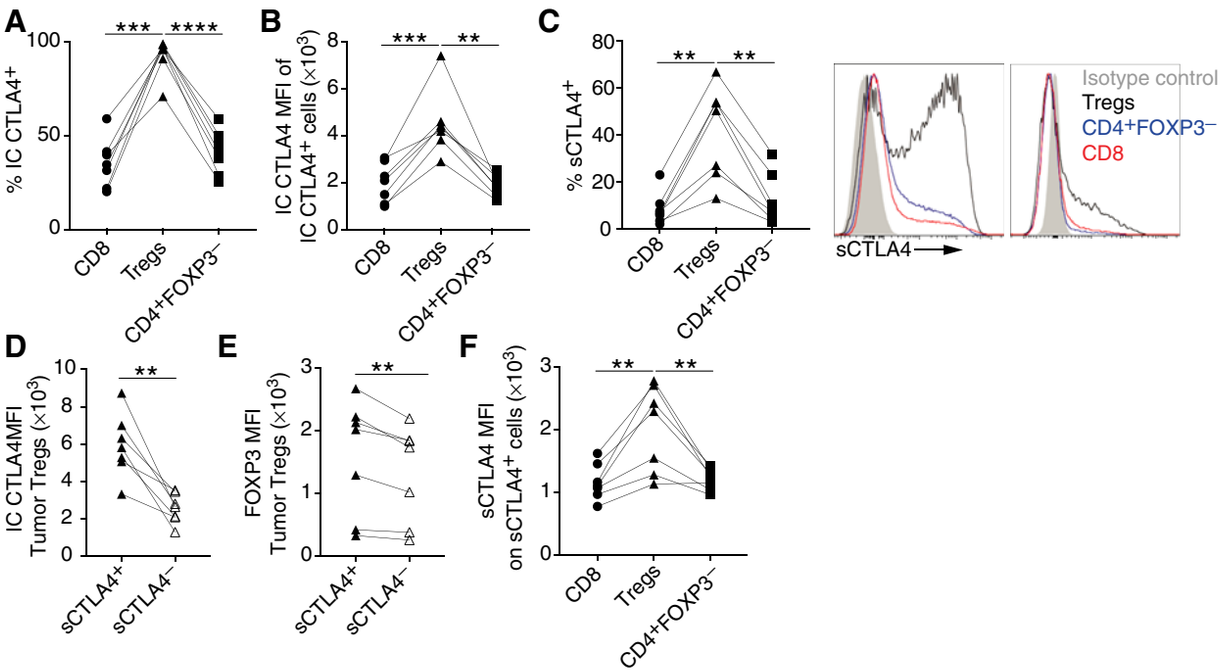

Figure 2.

Expression of sCTLA-4 of T-cell subsets infiltrating patient-derived NSCLC tissue. Single-cell suspensions from fresh patient-derived NSCLC tissue were analyzed by flow cytometry. **A,** Graph shows the frequency of intratumoral $CD8^+$ T cells, Tregs ($CD4^+FOXP3^+$), and $CD4^+FOXP3^-$ T cells (live $CD45^+CD20^-CD14^-CD11c^-CD66b^-CD3^+$) that expressed IC CTLA-4. **B,** Graph shows IC CTLA-4 expression by the IC CTLA-4^+ fraction of these intratumoral T-cell subsets. **C,** Graph shows the frequency of intratumoral $CD8^+$ T cells, Tregs, and $CD4^+FOXP3^-$ T cells that expressed surface CLTA4 (sCTLA-4, left). Representative histograms of the two types of sCTLA-4 expression patterns seen (Tregs, black histogram; $CD4^+FOXP3^-$ T cells, blue histogram; $CD8^+$ T cells, red histogram, right). Graphs show IC CTLA-4 (**D**) and FOXP3 (**E**) expression by sCTLA-4^+ and sCTLA-4^- intratumoral Tregs. **F,** Graph shows sCTLA-4 expression by the sCTLA-4^+ fraction of these intratumoral T-cell subsets. To determine statistical significance paired Student *t* tests were used (**, $P < 0.01$; ***, $P < 0.001$; ****, $P < 0.0001$).

circulating Tregs from matched patient blood, we found that both the frequency of sCTLA-4^+ Tregs and the intensity of sCTLA-4 expression were higher on Tregs infiltrating patient-derived NSCLC tissue compared with circulating Tregs from matched patient blood (Fig. 3C and D).

To begin to understand factors that contribute to higher sCTLA-4 on intratumoral compared with circulating Tregs, we evaluated IC CTLA-4 and FOXP3 in sCTLA-4^+ and sCTLA-4^- Tregs infiltrating the tumor and in circulation. Although sCTLA-4^+–circulating Tregs expressed more IC CTLA-4 than sCTLA-4^- circulating Tregs (Fig. 3E), they expressed less IC CTLA-4 compared with intratumoral sCTLA-4^+ Tregs (Fig. 3F). Likewise, whereas sCTLA-4^+–circulating Tregs expressed more FOXP3 than sCTLA-4^- circulating Tregs (Fig. 3G), these Tregs had lower FOXP3 than intratumoral sCTLA-4^+ Tregs (Fig. 3H). These data suggest that the amount of sCTLA-4 on sCTLA-4^+ Tregs reflects the cell's microenvironment, the total expression of CTLA-4, and also associates with the amount of FOXP3 expression.

Expression of sCTLA-4 by T cells infiltrating patient-derived melanoma tissue

Using flow cytometry, we found that in a majority of patient-derived melanoma tissue a greater frequency of Tregs expressed sCTLA-4 than conventional $CD4^+$ T cells from the same tissue (Fig. 4A). Furthermore, as with Tregs infiltrating patient-derived NSCLC tissue, sCTLA-4^+ Tregs infiltrating patient-derived melanoma tissue expressed significantly more sCTLA-4 on a per cell basis compared with sCTLA-4^+ $CD8^+$ or $CD4^+$ effector T cells from the same tumor tissue (Fig. 4B). As for Tregs infiltrating NSCLC, sCTLA-4^+ Tregs infiltrating patient-derived melanoma tissue expressed more FOXP3 and IC CTLA-4 than sCTLA-4^- Tregs from the same samples (Fig. 4C and D).

Higher intratumoral CD56 expression associates with benefit from ipilimumab

Productive depletion of intratumoral Tregs may enhance the efficacy of anti–CTLA-4 in patients. In a murine model we found that depletion of intratumoral Tregs following administration of anti–CTLA-4 coincided with activation and degranulation of NK cells. Thus, a possibility was that patients with higher frequencies of intratumoral NK cells may be more likely to benefit from anti–CTLA-4 therapies. In support of this model, analysis of available RNA-seq data (20) revealed that higher intratumoral CD56 (*NCAM1*) expression was associated with benefit from ipilimumab in patients with cutaneous melanoma (Fig. 4E).

Anti–CTLA-4 plus IL15/IL15Rα complexes enhance tumor control

Anti–CTLA-4 activated intratumoral NK cells coincident to intratumoral Treg depletion in the CT26 model (Fig. 1A–E),

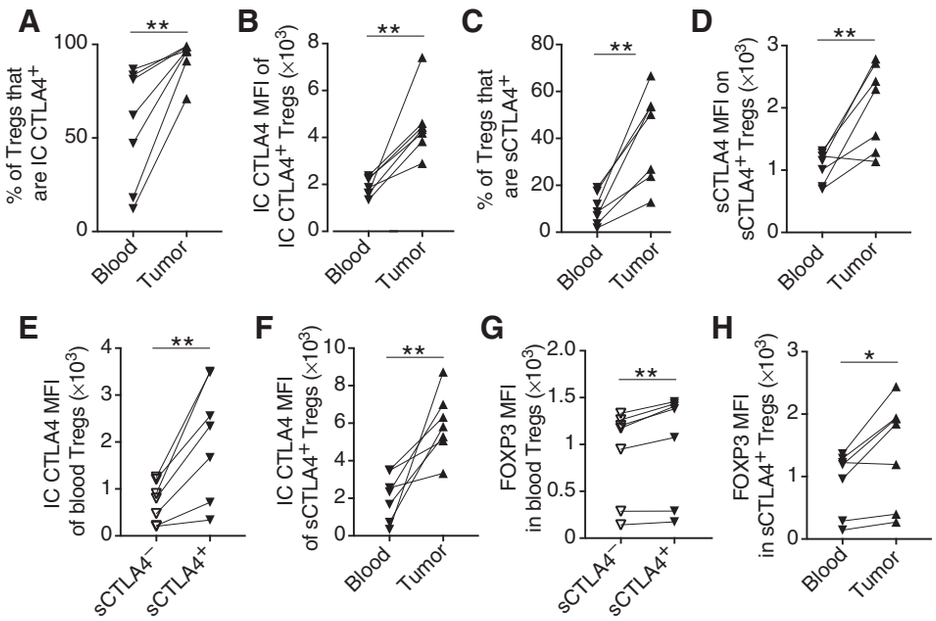

Figure 3.

Tregs infiltrating patient-derived NSCLC tissue have higher expression of sCTLA-4 compared with peripheral Tregs. Comparison of T-cell subsets from patient-derived NSCLC tissue (from Fig. 2) with T-cell subsets in matched patient blood collected the morning of biopsy. **A,** Graph shows the frequency of circulating and intratumoral Tregs ($CD4^+FOXP3^+$) that expressed IC CTLA-4. **B,** Graph shows IC CTLA-4 expression by the IC CTLA-4^+ fraction of circulating and intratumoral Tregs. **C,** Graph shows the frequency of circulating and intratumoral Tregs that expressed sCTLA-4. **D,** Graph shows sCTLA-4 expression by the sCTLA-4^+ fraction of circulating and intratumoral Tregs. **E,** Graph shows IC CTLA-4 expression by circulating sCTLA-4^+ or sCTLA-4^- Tregs. **F,** Graph shows IC CTLA-4 expression by circulating or intratumoral sCTLA-4^+ Tregs. **G,** Graph shows FOXP3 expression by circulating sCTLA-4^+ or sCTLA-4^- Tregs. **H,** Graph shows FOXP3 expression by circulating or intratumoral sCTLA-4^+ Tregs. To determine statistical significance paired Student *t* tests were used (*, $P < 0.05$; **, $P < 0.01$).

and intratumoral expression of the NK-cell marker, CD56, was increased in patients with cutaneous melanoma who benefited from ipilimumab. Thus, a possibility was that therapies that enhance intratumoral NK cells may synergize with anti–CTLA4 therapy. To test this possibility, mice bearing CT26 tumors were treated with anti–CTLA-4 (clone 9D9), IL15/IL15Rα complexes (containing 0.5 μg human IL15 and 2.33 μg of soluble murine IL15Rα-Fc per dose; ref. 21), which have been shown to increase intratumoral NK cells (22), or combination therapy. As expected, anti–CTLA-4 monotherapy moderately limited tumor progression, but, in this model, monotherapy with IL15/IL15Rα complexes was ineffective. However, combination therapy with anti–CTLA-4 plus IL15/IL15Rα complexes enhanced tumor control compared with either monotherapy (Fig. 4F).

Discussion

We showed that Tregs infiltrating murine tumors, as well as patient-derived tumors preferentially expressed sCTLA-4. Consistently, anti–CTLA-4 specifically depleted intratumoral Tregs in an FcR-dependent manner. We further found that anti–CTLA-4 therapies induced NK-cell activation and degranulation particularly in the tumor microenvironment, and this corresponded with anti–CTLA-4–mediated depletion of intratumoral Tregs. Moreover, increased intratumoral CD56 expression was associated with benefit from ipilimumab, and in a murine model anti–CTLA-4 plus IL15/IL15Rα complexes enhanced tumor control compared with either monotherapy. Thus enhanced intratumoral NK-cell activity may contribute to the efficacy of anti–CTLA-4 therapy.

Our data suggest that anti–CTLA-4 opsonizing intratumoral Tregs leads to activation of FcR^+ cells, including NK cells, which can then mediate ADCC of these anti–CTLA-4 opsonized Tregs. Thus, NK cells may contribute to anti–CTLA-4–mediated depletion of intratumoral Tregs (Supplementary Fig. S3). In agreement with this, NK cells have been shown to be able to mediate ADCC of CTLA-4^+ Tregs in the presence of a human CTLA-4 antibody (23). Alternatively, intratumoral Tregs may inhibit NK cells, and anti–CTLA-4–mediated depletion of intratumoral Tregs may indirectly allow for NK-cell activation and degranulation when these NK cells target tumor cells. This activation of NK cells following Treg depletion may contribute to the durable responses induced by anti–CTLA-4.

The cytokine IL15 supports NK-cell proliferation, survival, and cytolytic activity, and administration of IL15/IL15Rα complexes has been shown to enhance intratumoral NK-cell frequencies (22). Thus, although we do not rule out the likelihood that the effect of IL15/IL15Ra complexes on $CD8^+$ T cells contributes to the increased tumor control seen in mice cotreated with IL15 super agonists and anti–CTLA-4, our data suggest that increased intratumoral NK-cell frequencies and activity may be important for the synergy between IL15 complexes and anti–CTLA-4 in controlling tumor progression. Consistently, increased intratumoral amounts of the NK-cell marker CD56 was associated with benefit from ipilimumab in patients with cutaneous melanoma,

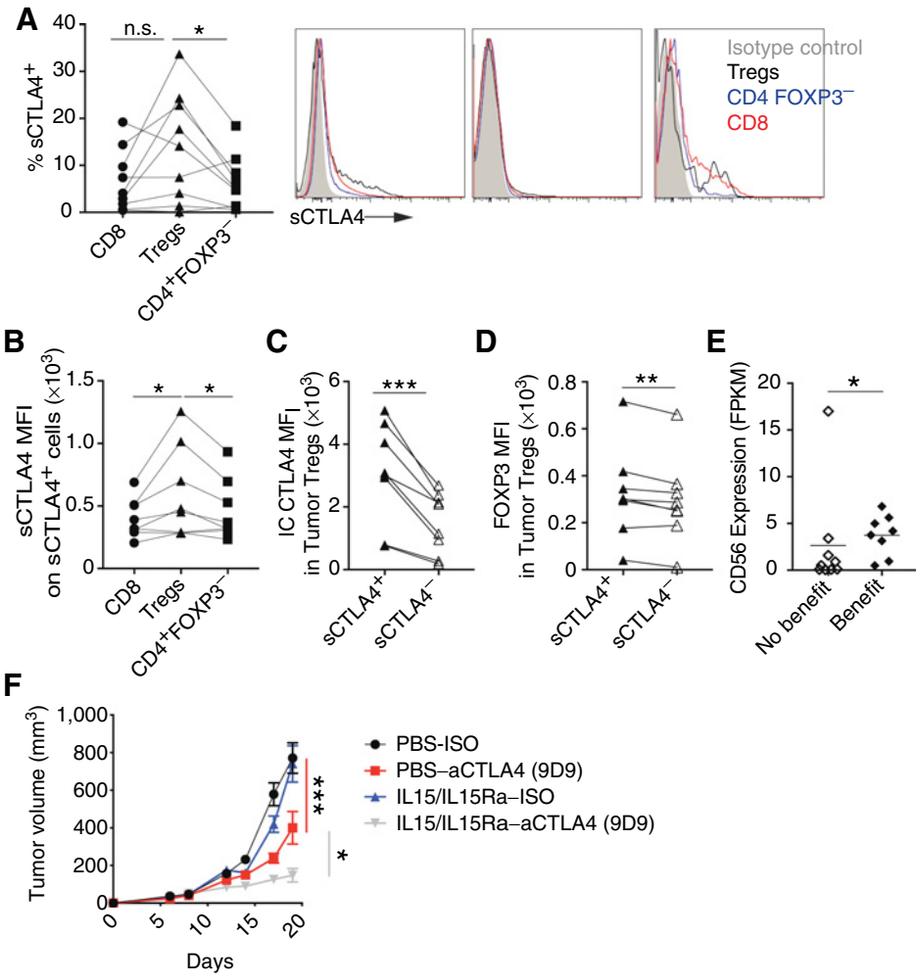

Figure 4.

Expression of sCTLA-4 on T-cell subsets infiltrating patient-derived melanoma tissue. Single-cell suspensions from fresh patient-derived melanoma tissue were analyzed by flow cytometry. **A,** Graph shows the frequency of intratumoral $CD8^+$ T cells, Tregs ($CD4^+FOXP3^+CD127^{lo}$), and $CD4^+FOXP3^-$ T cells that expressed sCTLA-4 (left). Histograms of sCTLA-4 expression on T cell (live $CD45^+CD20^-CD14^-CD11c^-CD66b^-CD3^+$) subsets from three of the patient-derived melanoma tissues (isotype control, filled gray histogram; Tregs, black histogram; $CD4^+FOXP3^-$, blue histogram; $CD8^+$ T cells, red histogram; right). **B,** Graph shows the expression (MFI) on indicated sCTLA-4^+ cells. Graphs show IC CTLA-4 (**C**), or FOXP3 (**D**) expression by intratumoral sCTLA-4^+ or sCTLA-4^- Tregs ($CD4^+FOXP3^+CD127^{lo}$) as determined by flow cytometry. **E,** Relative expression of CD56 (*NCAM1*) in cutaneous melanoma samples from patients with benefit or minimal or no benefit from ipilimumab as published by Snyder and colleagues (2014). **F,** Mice bearing CT26 tumors were treated with ± anti–CTLA-4 (clone 9D9, days 9, 12, 15, and 17) ± IL15/IL15Rα complexes (days 6 and 8, containing 0.5 μg human IL15 and 2.33 μg of soluble murine IL15Rα-Fc per dose), and tumor progression was followed (data shown is from one experiment with 10 mice per group). To determine statistical significance, paired Student *t* tests were used. For nonnormally distributed data, Wilcoxon rank-sum test was used to determine statistical significance. The trends of mean tumor volume over time were compared between groups using a linear mixed effects model with mouse as the random effect. A likelihood ratio testing nested models was used to examine whether slopes were significantly different between groups and overall (n.s., nonsignificant; *, $P < 0.05$; **, $P < 0.01$; ***, $P < 0.001$).

further suggesting that increased intratumoral NK cells enhance anti–CTLA-4 efficacy.

The ability of ipilimumab to deplete intratumoral Tregs in patients remains controversial. Although a decrease in intratumoral Tregs following ipilimumab treatment may correlate with efficacy in patients (12, 14), circulating Tregs are not decreased following administration of anti–CTLA-4 (11–13). We found that surface CTLA-4 expression was enhanced on Tregs infiltrating patient-derived tumor tissue compared with circulating Tregs from matched patient blood. These data provide a potential rationale for why anti–CTLA-4 therapy has been found to specifically reduce intratumoral but not circulating Tregs in patients. Thus, anti–CTLA-4 therapies may preferentially deplete intratumoral Tregs in patients, and specifically intratumoral Tregs with enhanced expression of not only CTLA-4 but also FOXP3.

In conclusion, we showed that anti–CTLA-4 therapy induced activation and degranulation of intratumoral NK cells and that combination therapy with IL15/IL15Rα complexes enhanced tumor control. In addition, increased intratumoral amounts of the NK-cell marker CD56 was associated with benefit from ipilimumab in patients with advanced cutaneous melanoma.

Nonetheless, it remains to be determined whether NK cells contribute to anti–CTLA-4–mediated Treg depletion and the enhanced tumor control induced by combination therapy with anti–CTLA-4 plus IL15/IL15Rα complexes. Thus, future research should investigate the role of NK cells in anti–CTLA-4 efficacy and whether increased intratumoral NK cell numbers enhance anti–CTLA-4 efficacy.

Disclosure of Potential Conflicts of Interest

R.K. Amaravadi has ownership interest (including stock, patents, etc.) in Pinpoint Therapeutics and Immunaccel and is a consultant/advisory board member for Sprint Biosciences. M.J. Turk has ownership interest (including stock, patents, etc.) in Celdara Medical, LLC. L.M. Schuchter has provided expert testimony for DLA piper. T.C. Mitchell is a consultant/advisory board member for Merck, BMS, Incyte, Aduro, and Regeneron. E.L. Stone is director of immune-oncology at and has ownership interest (including stock, patents, etc.) in GigaGen, Inc. M.P. Rubinstein reports receiving commercial research funding from Altor Bioscience and XOMA, and has ownership interest (including stock, patents, etc.) in XOMA. No potential conflicts of interest were disclosed by the other authors.

Authors' Contributions

Conception and design: E. Sanseviero, M.P. Rubinstein, T.C. Mitchell, E.L. Stone

Development of methodology: E. Sanseviero, E.M. O'Brien, M.P. Rubinstein, T.C. Mitchell

Acquisition of data (provided animals, acquired and managed patients, provided facilities, etc.): E. Sanseviero, E.M. O'Brien, J.R. Karras, T.B. Shabaneh, W. Xu, C. Zheng, X. Xu, G.C. Karakousis, R.K. Amaravadi, B. Nam, M.J. Turk, L.M. Schuchter, T.C. Mitchell, E.L. Stone

Analysis and interpretation of data (e.g., statistical analysis, biostatistics, computational analysis): E. Sanseviero, E.M. O'Brien, T.B. Shabaneh, B.A. Aksoy, X. Yin, R.K. Amaravadi, M.P. Rubinstein, Q. Liu, E.L. Stone

Writing, review, and/or revision of the manuscript: E. Sanseviero, E.M. O'Brien, J.R. Karras, T.B. Shabaneh, W. Xu, X. Xu, G.C. Karakousis, R.K. Amaravadi, B. Nam, M.J. Turk, T.C. Mitchell, Q. Liu, E.L. Stone

Administrative, technical, or material support (i.e., reporting or organizing data, constructing databases): T.B. Shabaneh, W. Xu, C. Zheng, B. Nam, J. Hammerbacher, M.P. Rubinstein

Study supervision: E.L. Stone

Acknowledgments

The authors are grateful to Sophia Simon, Autumn Powell, Keira McAfee, and Claire Cohen (Wistar) for genotyping and mouse line maintenance assistance. The authors thank Patricia Swanson and Lori Huelsenbeck-Dill (HFGCC-Christiana Health Care System) for assistance with patient recruitment. The authors are especially grateful for scientific discussions with the Stone Lab and members of The Wistar Institute. This research was sponsored by The Wistar Institute Cancer Center and an American Cancer Society-IRG grant. The research was funded by a Bristol-Myers Squibb-MRA Young Investigator Award (to E.L. Stone), a Wistar/UPenn Specialized Program of Research Excellence grant in Skin Cancers Developmental Research Award (to E.L. Stone), and a grant from BNY Mellon Wealth Management through The Martha W. Rogers Charitable Trust (to E.L. Stone). E.L. Stone was funded in part by the Emerson Collective, 1K01DK095008 (NIDDK), and a PA CURE grant. J.R. Karras was funded in part by a PENNPort IRACDA postdoctoral fellowship. E. Sanseviero was funded in part by a Fellowship from Istituto Pasteur Italia–Fondazione Cenci Bolognetti. Core Facilities were supported by Cancer Center Support Grant CA010815 to The Wistar Institute. B.A. Aksoy and J. Hammerbacher are supported in part by MUSC. M.J. Turk and T.B. Shabaneh are supported by NIH grants R21CA209375-01, R01CA225028, and R01CA205965. The authors are grateful for support from The Tara Miller Melanoma Foundation.

The costs of publication of this article were defrayed in part by the payment of page charges. This article must therefore be hereby marked *advertisement* in accordance with 18 U.S.C. Section 1734 solely to indicate this fact.

Received June 11, 2018; revised February 2, 2019; accepted June 18, 2019; published first June 25, 2019.

References

1. Wolchok JD, Chiarion-Sileni V, Gonzalez R, Rutkowski P, Grob JJ, Cowey CL, et al. Overall survival with combined nivolumab and ipilimumab in advanced melanoma. N Engl J Med 2017;377:1345–56.
2. Long GV, Atkinson V, Lo S, Sandhu S, Guminski AD, Brown MP, et al. Combination nivolumab and ipilimumab or nivolumab alone in melanoma brain metastases: a multicentre randomised phase 2 study. Lancet Oncol 2018;19:672–81.
3. Motzer RJ, Tannir NM, McDermott DF, Aren Frontera O, Melichar B, Choueiri TK, et al. Nivolumab plus ipilimumab versus sunitinib in advanced renal-cell carcinoma. N Engl J Med 2018;378:1277–90.
4. Hellmann MD, Ciuleanu TE, Pluzanski A, Lee JS, Otterson GA, Audigier-Valette C, et al. Nivolumab plus ipilimumab in lung cancer with a high tumor mutational burden. N Engl J Med 2018;378:2093–104.
5. Simpson TR, Li F, Montalvo-Ortiz W, Sepulveda MA, Bergerhoff K, Arce F, et al. Fc-dependent depletion of tumor-infiltrating regulatory T cells co-defines the efficacy of anti-CTLA-4 therapy against melanoma. J Exp Med 2013;210:1695–710.
6. Bulliard Y, Jolicoeur R, Windman M, Rue SM, Ettenberg S, Knee DA, et al. Activating Fc γ receptors contribute to the antitumor activities of immunoregulatory receptor-targeting antibodies. J Exp Med 2013;210:1685–93.
7. Selby MJ, Engelhardt JJ, Quigley M, Henning KA, Chen T, Srinivasan M, et al. Anti-CTLA-4 antibodies of IgG2a isotype enhance antitumor activity through reduction of intratumoral regulatory T cells. Cancer Immunol Res 2013;1:32–42.
8. Arce Vargas F, Furness AJS, Litchfield K, Joshi K, Rosenthal R, Ghorani E, et al. Fc effector function contributes to the activity of human anti-CTLA-4 antibodies. Cancer Cell 2018;33:649–63.
9. Ingram JR, Blomberg OS, Rashidian M, Ali L, Garforth S, Fedorov E, et al. Anti-CTLA-4 therapy requires an Fc domain for efficacy. Proc Natl Acad Sci U S A 2018;115:3912–7.
10. Du X, Tang F, Liu M, Su J, Zhang Y, Wu W, et al. A reappraisal of CTLA-4 checkpoint blockade in cancer immunotherapy. Cell Res 2018;28:416–32.
11. Kavanagh B, O'Brien S, Lee D, Hou Y, Weinberg V, Rini B, et al. CTLA4 blockade expands FoxP3+ regulatory and activated effector CD4+ T cells in a dose-dependent fashion. Blood 2008;112:1175–83.
12. Tarhini AA, Edington H, Butterfield LH, Lin Y, Shuai Y, Tawbi H, et al. Immune monitoring of the circulation and the tumor microenvironment in patients with regionally advanced melanoma receiving neoadjuvant ipilimumab. PLoS One 2014;9:e87705.
13. Furness AJS, Vargas FA, Peggs KS, Quezada SA. Impact of tumour microenvironment and Fc receptors on the activity of immunomodulatory antibodies. Trends Immunol 2014;35:290–8.
14. Romano E, Kusio-Kobialka M, Foukas PG, Baumgaertner P, Meyer C, Ballabeni P, et al. Ipilimumab-dependent cell-mediated cytotoxicity of regulatory T cells ex vivo by nonclassical monocytes in melanoma patients. Proc Nat Acad Sci U S A 2015;112:6140–5.
15. Stojanovic A, Fiegler N, Brunner-Weinzierl M, Cerwenka A. CTLA-4 is expressed by activated mouse NK cells and inhibits NK Cell IFN-gamma production in response to mature dendritic cells. J Immunol 2014;192:4184–91.
16. Crawford A, Angelosanto JM, Kao C, Doering TA, Odorizzi PM, Barnett BE, et al. Molecular and transcriptional basis of $CD4^+$ T cell dysfunction during chronic infection. Immunity 2014;40:289–302.
17. Linsley PS, Bradshaw J, Greene J, Peach R, Bennett KL, Mittler RS. Intracellular trafficking of CTLA-4 and focal localization towards sites of TCR engagement. Immunity 1996;4:535–43.

18. Meeth K, Wang JX, Micevic G, Damsky W, Bosenberg MW. The YUMM lines: a series of congenic mouse melanoma cell lines with defined genetic alterations. Pigment Cell Melanoma Res 2016;29: 590–7.
19. Leung HT, Bradshaw J, Cleaveland JS, Linsley PS. Cytotoxic T lymphocyte-associated molecule-4, a high-avidity receptor for CD80 and CD86, contains an intracellular localization motif in its cytoplasmic tail. J Biol Chem 1995;270:25107–14.
20. Snyder A, Makarov V, Merghoub T, Yuan J, Zaretsky JM, Desrichard A, et al. Genetic basis for clinical response to CTLA-4 blockade in melanoma. N Engl J Med 2014;371:2189–99.
21. Doedens AL, Rubinstein MP, Gross ET, Best JA, Craig DH, Baker MK, et al. Molecular Programming of Tumor-Infiltrating CD8+ T cells and IL15 resistance. Cancer Immunol Res 2016;4:799–811.
22. Epardaud M, Elpek KG, Rubinstrain MP, Yonekura A, Bellemare-Pelletier A, Bronson R, et al. Interleukin-15/interleukin-15Ra complexes promote destruction of established tumors by reviving tumor-resident CD8+ T cells. Cancer Res 2008;68:2972–83.
23. Gombos RB, Gonzalez A, Manrique M, Chand D, Savitsky D, Morin B, et al. Toxicological and pharmacological assessment of AGEN1884, a novel human IgG1 anti-CTLA-4 antibody. PLoS One 2018;13: e0191926.